Transitional natural convection flow in a vertical channel: Impact of the external thermal stratification

Martin Thebault, Stéphanie Giroux-Julien, Victoria Timchenko, Christophe Menezo, John Reizes

Highlights

Transitional natural convection flow in a vertical channel: Impact of the external thermal stratification

Martin Thebault, Stéphanie Giroux–Julien, Victoria Timchenko, Christophe Ménézo, John Reizes

- Impact of positive thermal stratification on the flow is studied experimentally
- Impact of negative and positive stratification is investigated numerically
- External thermal stratification displaces the transition of the flow
- Excellent agreements are obtained with theoretical model of the literature

Transitional natural convection flow in a vertical channel: Impact of the external thermal stratification

Martin Thebault[a,b], Stéphanie Giroux–Julien[a], Victoria Timchenko[b], Christophe Ménézo[c], John Reizes[b]

[a] *Univ Lyon, CNRS, INSA-Lyon, Université Claude Bernard Lyon 1, CETHIL UMR5008, F-69621, Villeurbanne, France*
[b] *School of Mechanical and Manufacturing Engineering, UNSW-Sydney, Sydney 2052, Australia*
[c] *University Savoie Mont-Blanc, LOCIE UMR CNRS 5271, Campus Scientifique Savoie Technolac – F-73376, Le Bourget-du-Lac, France*

Abstract

The impact of the external thermal stratification on the flow behavior and the mass flow rate in an open ended vertical channel with one side uniformly heated is investigated experimentally and numerically. Both experimental and numerical studies show that the increase of the external stratification lowers the velocity and the mass flow rate but also displaces the transition height at a lower location in the channel. The numerical model was used to study the cases of weak and negative thermal stratifications which are barely achievable in non-controlled experimental laboratory conditions but are common in the atmosphere. Different flow regimes are identified with flow being fully laminar when the stratification is weak or negative and flow being transitional to turbulent for higher stratifications. Finally, the numerically obtained mass flow rates with the various external thermal stratifications are shown to be in excellent agreement with a theoretical model developed in a previous work.

Keywords:
transitional natural convection, external thermal stratification, experimental, numerical, chimney effect

Email address: martin.thebault@univ-smb.fr (Martin Thebault)

1. Introduction

The problem of natural convection in vertical systems has been the object of a constant interest for more than 50 years. At first applications were nuclear or cooling of electronic component [1], studies or buoyant flows in shafts [2], for fire hazard safety [3] or for building ventilation [4], [5]. More recently, research on natural convection has benefited from the renewal of the interest for the harvesting of solar energy. As a result, among other technologies, ventilated photovoltaic arrays integrated in buildings (BIPV,PVT) have been developed. These components use direct radiation from the sun to generate electricity, whilst the concomitant, but unwanted thermal heating of the arrays generates natural convective flows in the space between the photovoltaic array and the wall enclosing the building. This natural ventilation cools down the photovoltaic arrays, thereby increasing their efficiency [6], with the added advantage that the flow can also be used for the heating of the building during the day or for cooling it at night.

The study of such system is challenging for several reasons. When ventilated BIPV systems operate in real-conditions, the flow is expected to be transitional or turbulent. Moreover, it is impacted by the environment, which significantly increases the complexity of the problem. Therefore, laboratory-scale experiments and numerical models usually take the aspect of a heated vertical channel which represents a simplification of the problem.

Natural convective flows observed in experimental channels and in numerical simulations of channels of finite sizes often display the following characteristics:

1. The flow is spatially developing over a large region;
2. The flow undergoes a transition from a laminar to a turbulent regime.
3. Experimentally the flow is submitted to various external factors such as external thermal stratification or ambient velocity disturbances. These factors impact the flow spatial development as well as the transitional process.

In a recent paper Thebault et al. [7] provided a detailed description of the spatial development of the transitional flow and associated different indicators to different stages of the transition. In the present paper, the effect of the boundary conditions, and more especially the external thermal stratification, on the transitional flow is investigated.

The impact of the ambient temperature distribution on natural convection has been known for some time and has been extensively studied for

heated vertical plates. In 1967, Cheesewright [8] first developed similarity solution for steady laminar natural convective flows adjacent to vertical isothermal plate in non-uniform ambient temperatures. His work was motivated after he noticed significant differences between analytical models and experimental measurements which he attributed to the external thermal stratification.

Another pioneering experimental and theoretical study of Jaluria and Gebhart [9] investigated the effect of external thermal stratification on a natural convection flow induced by a uniformly heated vertical plate. They used a stratification factor that they obtained by similarity analysis to quantify the stratification strength. Among different observations they observed that as the external thermal stratification was increasing the velocity was decreasing. They reasoned that this was caused by the fact that as the ambient temperature increases downstream, the temperature difference between the local ambient temperature at a particular elevation and the temperature of the upward moving fluid in the boundary layer at the same elevation is less than it would have been if the ambient temperature had been uniform, resulting in a reduced buoyancy and therefore, to lower induced velocities. They also noticed that as the surrounding thermal stratification increased, the transition height was moved at a higher location downstream which they attributed to a stabilization of the flow, inherent to the increase in thermal stratification.

Despite natural convection vertical plate flows share some similitude with vertical channel flows; these two flows remains very different, regarding their velocity and thermal quantities as well as the transitional behavior (see e.g. [10, 11]). That is why the direct comparison between these flows may be limited and must be carried with caution.

Only few studies were carried out on the impact of the external thermal stratification in the case of a uniformly heated vertical channel. Regarding the previous numerical works, the impact of the ambient temperature distribution was observed in some cases in which the channel was modeled inside of a cavity with adiabatic external boundary conditions, the fluid being initially at uniform temperature [12, 13, 14]. Because of the heat injection in the channel, the top of the cavity became progressively thermally stratified and once the developing thermal stratification reached the top of the channel, the velocity in the channel decreased. More recently the impact of thermal stratification was explicitly studied in a laminar two-dimensional numerical investigation by Ramalingom et al. [15] which confirmed the previous obser-

vations.

Experimentally the impact of the temperature stratification on the mass flow rate had been known for many years though not specifically investigated. Haaf et al. [16] in a pilot project on a solar chimney, underlined and recorded its "favourable or unfavourable effect", referring to respectively negative and positive thermal stratifications, both of them being encountered in the first dozens meters of the atmosphere [17].

In a symmetrically heated water channel, Daverat et al. [18] highlighted that there is a strong influence of the external thermal stratification on the velocity and thermal fields of the flow. They observed thermal stratifications up to 9 K/m for a fixed heat input of 190 W/m^2. Later on, in a scaling analysis on the same configuration, Li et al. [19] evaluated that the external thermal stratification should generate a pressure drop at the boundaries in the same order of magnitude as the driving pressure generated by buoyancy therefore concluding on a potential high effect of it on the flow. Recently, Thebault et al. [20] have undertaken experimental and theoretical studies in a one-side heated air channel and showed that the external thermal stratification was greatly impacting the mass flow rate. They proposed a theoretical model in order to predict the convective mass flow rate in a thermally stratified ambient.

However, in the great majority of the experimental studies, when the external thermal stratification is mentioned, the problem that it induces was gotten around. Either its impact is assumed to be neglectible [21], or the measurements are done before the surrounding atmosphere becomes stratified, or they are carried out under a constant external thermal stratification [22]. Sometime an active cooling system is used in order to keep the ambient temperature uniform [23, 24], but it requires extreme caution in order not to disturb the flow.

As mentioned above, Jaluria and Gebhart [9] found that the external thermal stratification had an influence on the transitional behaviour of the flow in the case of a vertical plate. However, no works were undertaken to study this phenomenon in the vertical open ended channel.

Therefore, the present paper is focusing on the effects of the external thermal stratification on a three-dimensional spatially-developing transitional natural convective flow induced by a uniform heat flux on one side in a vertical channel of finite size. The effect of the external thermal stratification on the flow behavior is studied using both experimental and numerical data. The numerical model is then used to study the effect of weak and neg-

ative stratifications on the flow. Finally the numerically computed mass flow rate obtained for the negative and positive external thermal stratifications, is compared to the theoretical predictive model of Thebault et al. [20].

2. Methodology

This study is in the continuation of the works of Thebault et al. [20, 7] in which the configuration studied as well as the experimental and numerical methodologies are introduced in details. For those reasons, only a brief summary is presented here.

The Rayleigh number Ra, defined in terms of the heat flux, q (W/m^2), and on the height of the channel, H (m), is defined as the product of the Grashof number and the Prandtl number and can therefore be expressed as

$$Ra = \frac{gbqH^4}{a\nu\kappa}, \tag{1}$$

in which g (m/s^2) is the gravitational acceleration, b (1/K) is the coefficient of thermal expansion, ν (m^2/s) is the kinematic viscosity, κ (W/m·K) is the thermal conductivity of air and a (m^2/s) is the thermal diffusivity. Two injected heat flux of $q = 90$ W/m^2 and $q = 208$ W/m^2 are studied which correspond to Rayleigh numbers of $Ra = 1.5 \times 10^{12}$ and $Ra = 3.5 \times 10^{12}$.

2.1. Problem definition

The configuration studied consists in a vertical channel of height $H = 1.5$ m, depth $D = 0.1$ m and width $W = 0.7$ m, which is uniformly heated on one side. The notation and the coordinate system are presented in Fig. 1 (a).

The distribution of temperature in the room was measured and had a linear distribution [20], with the temperature increasing with height. Therefore the room temperature had a positive thermal stratification and could be expressed as a linear function of δ_T (K/m), the vertical temperature gradient in the room:

$$T_a(y) = T_0 + (y - y_0)\,\delta_T. \tag{2}$$

The subscript 0 stands for reference a quantity taken at the height of the inlet level, $y_0 = 0$, far from the channel as illustrated in Fig. 1 (a) with T_0. The subscript a refers to a quantity taken in the far-field, and δ_T is the temperature gradient in the far-field. The external temperature gradient δ_T

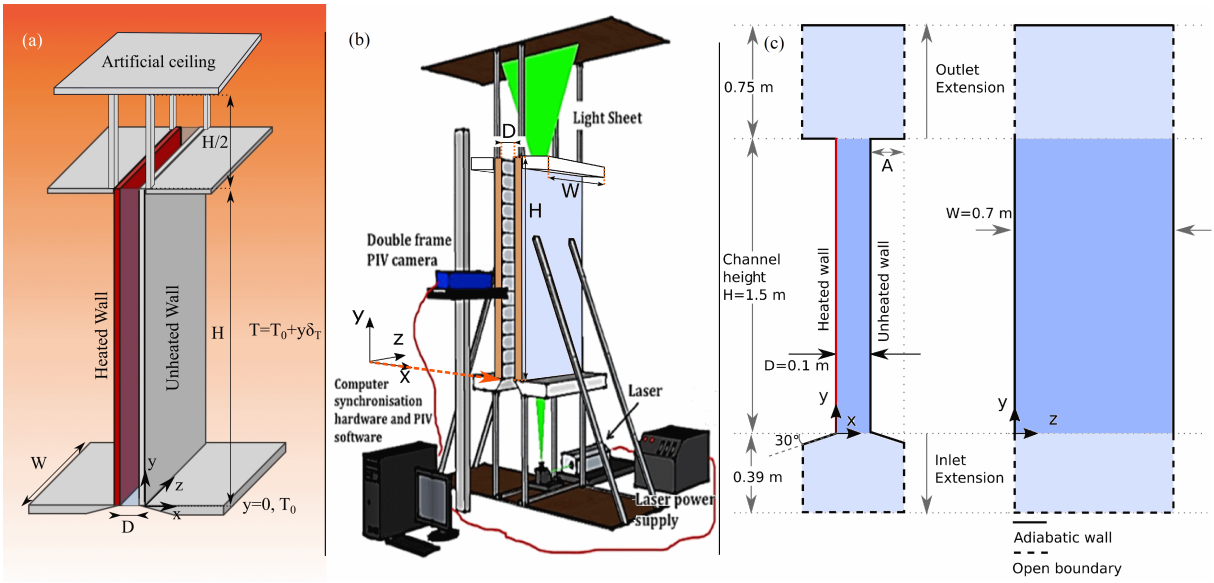

Figure 1: (a) Scheme of the configuration studied. The background color illustrates the ambient thermal stratification. (b) Scheme of the experimental apparatus and PIV measurement devices, (c) scheme of the computational domain

is positive if the temperature increases upwards and negative if it decreases. This stratification is illustrated by the background color in Fig. 1.

In these conditions, the hydrostatic pressure, p (Pa) in the thermally stratified far field can be expressed, using the perfect gas law, as [7]

$$p_a(y) = p_0 \left(1 + \frac{\delta_T}{T_0}\left(y - y_0\right)\right)^{\frac{-g}{R_{air}\delta_T}}, \tag{3}$$

in which R_{air} (J/kg^{-1}K^{-1}) is the specific gas constant of air.

2.2. Experimental methodology

The experimental apparatus is represented in Fig.1 (b). Temperature measurements were carried with K-types thermocouples. They took place in the room, at the heated wall and in the fluid, at the inlet and the outlet of the channel. Experimental velocity measurements were conducted in the mid-plan $z/W = 0.5$ obtained with Particle Image Velocimetry (PIV) methodology. The PIV system consisted of a pulsed Nd: YAG laser emitting at 532 nm. A standard set of lenses was used to transform the laser beam

into a light sheet and a Charge-Coupled Device (CCD) with a resolution of 540×2048 pixels was used for image acquisition. The acquisition window corresponded to a 100 mm wide by 380 mm high section of the flow. As a consequence, the measurement in the different regions of the channel could not have been performed simultaneously.

The external thermal stratification occurred naturally in the laboratory, mainly due to the heating from the different elements of the apparatus. Therefore, sometimes, between different sets of experiments, the external thermal gradient δ_T changed. However changes of δ_T during one measurement were very small leading to non-appreciable differences of the flow quantities [20]. More details about the experimental measurements as well as the ambient conditions are presented in [20, 7]

2.3. Numerical methodology

The corresponding computational domain is presented in Fig.1 (c). It is composed of the channel itself and extended domains, before the channel inlet and above the channel outlet. This type of domain, defined as an I-type configuration by Manca et al. [25], allows the air to flow into and out of the channel.

The numerical model consisted in a three dimensional Large-Eddy-Simulation (LES) using a Vreman subgrid-scale model adapted to transitional natural convection [26, 27].

At the open boundaries of the computational domain Fig.1 (c), the thermal and pressure stratifications equations (2,3) inherent to a thermally stratified environment were modeled using a user-defined function. As was reported in numerous experimental studies (see e.g. [10, 28, 29]), there are large velocity disturbances at the inlet of the channel that comes from the surrounding environment. These disturbances must be considered to obtain a more realistic numerical model [30, 31, 7]. To mimic that environmental velocity disturbance, an inlet velocity noise was added at the lower open boundaries of the computational domain using the spectral synthesizer approach [32] which is commonly used in LES methodology [33]. Finally the wall to wall radiation that is observed in the experiments was taken into consideration numerically by distributing a part of the total injected heat flux on the unheated wall. More details about the numerical model, the boundary conditions and their validation is presented in Thebault et al. [7].

After mesh and extended domain size validations [7], the number of elements inside the channel itself was of 75×240×85 in the x, y and z directions

resulting in a maximum y-plus value of $x^+ = 0.8$ in the wall-normal direction. The horizontal size parameters of the extended domains were of A =14 cm at $Ra = 1.5 \times 10^{12}$ and A =21 cm at $Ra = 3.5 \times 10^{12}$ (Fig.1 (c)).

2.4. Indicators of transition

In the following, all the temperatures are expressed as the temperature elevation over the reference temperature T_0 and noted θ.

$$\theta = T - T_0 \tag{4}$$

The air properties are taken at T_0. In the numerical simulations T_0 = 293.15 K.

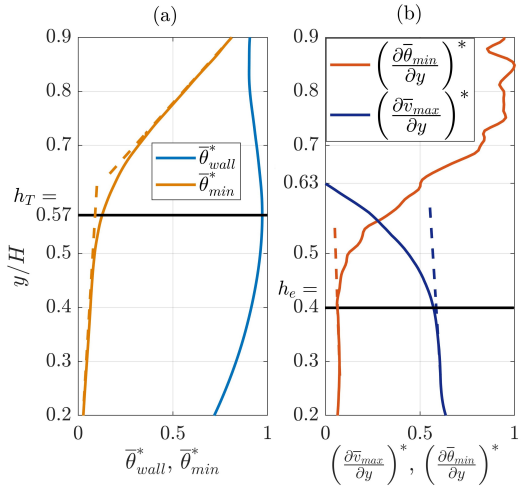

Figure 2: Representation of the indicators of transition and their determination for the present flow configuration at $Ra = 1.5 \times 10^{12}$. Streamwise evolution of (a) $\overline{\theta}^*_{wall}$ and $\overline{\theta}^*_{min}$, (b) $(\partial \theta_{min}/\partial y)^*$ and $(\partial v_{max}/\partial y)^*$. Thin dashed lines have been plotted to indicate linear trends or significant changes in the quantities growth. The transition indicator heights h_T and h_e have been indicated by thick black lines. Credit: [7]

To assess the transition behavior of the flow, different indicators of the transition have been used in the literature. These indicators were reviewed and presented for the case of the present configuration in Thebault et al. [7]. In the present paper, two indicators will be used. The first, h_e is defined based on changes of the streamwise growth of the the maximum velocity v_{max} (m/s) and the minimum fluid temperature θ_{min} (m/s), h_e indicates

early stages of the transition. The second indicator, h_T initially defined by Miyamoto et al. [10], is based on a local maximum of the temperature at the heated wall θ_{wall} and indicates an advanced stage of the transition.

These indicators are presented in Fig.2 for numerical results obtained with the present configuration at $Ra = 1.5 \times 10^{12}$. All the quantities were scaled with their maximum streamwise value for visualization purposes. The scaled quantities are indicated by the superscript $*$.

The indicator h_T attests a distinct separation of the evolution of the temperatures in the channel as from this height the temperature inside the channel considerably increases as can be seen with the evolution of θ_{min} in Fig.2 (a). The indicator h_e is located lower than h_T and is a relevant indicator to capture early changes in the wall-normal turbulent statistics which are characteristic of the turbulent transfers. The detailed spatial development of the flow around these indicators for this configuration is presented in Thebault et al. [7].

3. Effect of positive δ_T on the spatial development of the transitional flow.

The aim of this section is to study the effect of the external thermal stratification on the spatial development of the flow. For that purposes, numerical and experimental data will be used.

As was discussed in Thebault et al. [7], it is important to note that the agreement between the experimental and numerical results has never been reached in the literature for this type of configuration (see e.g. Fedorov and Viskanta [30], Lau et al. [31], Li et al. [34] or Tkachenko et al. [35]). The best reported agreements remain probably those of the numerical LES model of Lau et al. [36] with the experimental results of Miyamoto et al. [10]. In the present work, the same LES methodology is used, only the geometry was changed. Moreover reasonable agreements were obtained for the present configuration as was showed in Thebault et al. [7]. The ambition of the present paper is therefore not to achieve a better experimental-numerical agreement than those previously obtained. The ambition here is to assess and analyze similar trends between the experimental and numerical results about the influence of the external thermal stratification on the transitional flow.

The time-averaged experimental and numerical temperature distributions at the heated wall, $\overline{\theta}_{wall}$ at $z/W = 0.5$ are plotted at $Ra = 1.5 \times 10^{12}$ in re-

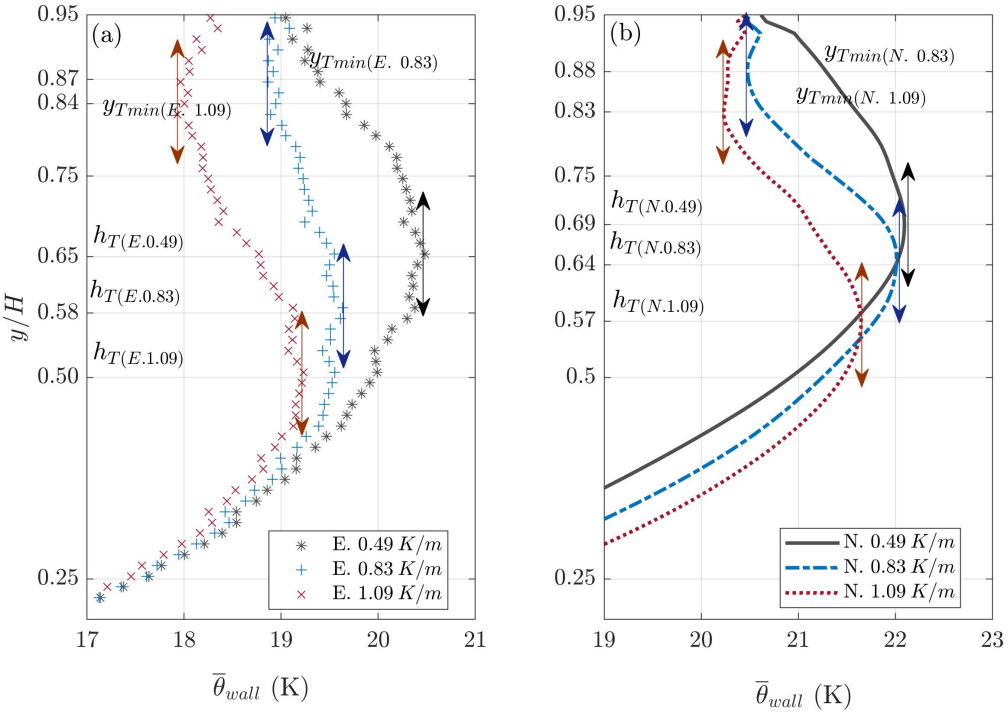

Figure 3: Temperature distribution at the wall at $Ra = 1.5 \times 10^{12}$, and three different external thermal stratifications $\delta_T = 0.49K/m$, $\delta_T = 0.83K/m$, $\delta_T = 1.09K/m$. (a) Experimental (E.), (b) Numerical (N.). Double headed arrows indicate the local maxima, h_T and minima y_{Tmin} of temperature

spectively Fig. 3 (a) and (b) for three different external thermal stratifications of δ_T =[0.49 K/m, 0.83 K/m, 1.09 K/m].

This type of temperature distribution at the heated wall has been widely described for the present configuration in the literature (see e.g. [7, 31, 21]), for that reason the focus will be here on the changes in the transition location identified here by h_T, defined in section 2.4.

In Fig. 3, h_T is identified by double headed arrows. Both experimentally and numerically, it can be observed that h_T and therefore the transition, is displaced at a lower location in the channel as the external thermal stratification increases. Moreover the value of the temperature maximum reached at h_T also decreases as the external thermal stratification increases. For the two higher stratifications, [0.83 K/m; 1.09 K/m], h_T is followed by a local mini-

mum of temperature, referred to as y_{Tmin}. This minimum of temperature is expected in uniformly heated configuration with a long enough channel. It indicates a late stage of the transition [7]. There is remarkable agreement in the trends showed by both experimental and numerical results. The detailed values of h_T, y_{Tmin} and $\overline{\theta}_{wall}(h_T)$ have been reported in Table 1.

Regarding the higher Rayleigh number at $Ra = 3.5 \times 10^{12}$ the values of h_T, y_{Tmin} and $\overline{\theta}_{wall}(h_T)$ have also been reported in Table 1 for three external thermal stratifications of δ_T =[0.31 K/m, 0.72 K/m, 1.33 K/m]. It appears that there are more differences between experimental and numerical data. However similar trends are observed regarding the displacement of the elevation of h_T and the decrease of the maximum temperature reached at the wall when the external thermal stratification increases.

It is interesting to note that in both the numerical and the experimental results, the transition moves lower in the channel as the external thermal stratification increases. This phenomenon is opposite to what was observed by Jaluria and Gebhart [9] with a uniform heat flux vertical plate and an explanation is provided in Appendix A.

Table 1: h_T, y_{Tmin} and $\overline{\theta}_{wall}(h_T)$ for the two investigated Rayleigh and three different external thermal stratifications

Ra	δ_T	Case	h_T	y_{Tmin}/H	$\overline{\theta}_{wall}(h_T)$ (K)
1.5×10^{12}	0.49	Exp	0.65	-	20.5
		Num	0.69	-	22.1
	0.83	Exp	0.58	0.87	19.6
		Num	0.64	0.84	22.0
	1.09	Exp	0.50	0.84	19.2
		Num	0.57	0.83	21.6
3.5×10^{12}	0.31	Exp	0.60	-	46.4
		Num	0.78	-	37.6
	0.72	Exp	0.57	-	43.6
		Num	0.70	-	37.0
	1.33	Exp	0.45	0.83	42.8
		Num	0.67	-	36.5

As mentioned in section 2.4 there is a change in the flow behavior at h_T characterized by an increase of the temperature in the bulk region. As a consequence, the changes of the location of h_T due to the external thermal

stratification are expected to also influence the outlet temperatures of the flow.

The outlet time-averaged fluid temperatures obtained in the mid-plane, at two different values [0.49 K/m; 1.09 K/m] of the stratifications at $Ra = 1.5 \times 10^{12}$, are plotted in Fig. 4. The temperature is high near the hot wall, and significantly lower the bulk of the flow. In the vicinity of the unheated wall, the slight temperature rise is due to the wall to wall radiation (see. [7]).

For the lower stratification the increase of temperature in the central region of the flow is in the range 2-4 K whereas for the higher stratification it is in the range 4-6 K. This difference can be explained by the fact that the transition have started lower in the channel for the higher stratification, resulting in more heat transferred from the wall to the bulk of the flow and therefore to a higher outlet temperature in the bulk region.

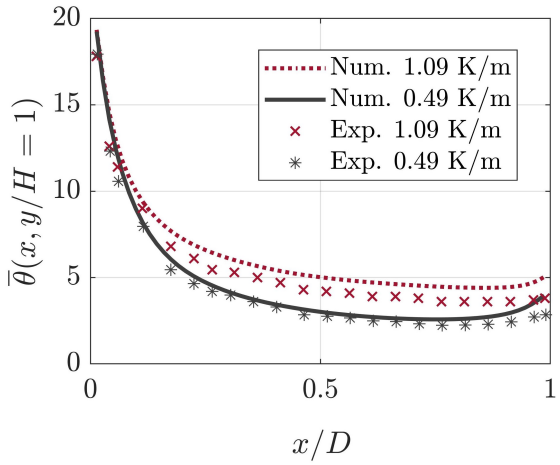

Figure 4: Temperature profiles at the outlet at $Ra = 1.5 \times 10^{12}$ $\delta_T = 0.49K/m$, $\delta_T = 1.09K/m$

The time-averaged streamwise velocities in the lower part of the channel ($y/H = 0.25$) and near the outlet ($y/H = 0.95$), in the mid-plane of the channel $z/W = 0.5$, are plotted in Fig. 5 for the two Rayleigh numbers and various external thermal stratifications.

At $y/H = 0.25$ the velocity profiles are composed of a high velocity buoyant region near the heated wall and a central region in which the velocity profiles are mainly flat. Based on the scaling analysis of Li et al. [19], and similarly to what was done for the present configuration in [7], the high

velocity region near the heated wall, in which the velocity in the streamwise direction is accelerated due to the heating of the flow, will be referred to as the natural convection boundary layer (NCBL). The central region, where the velocity profiles are flat and where the streamwise velocity is decelerated is referred to as the bulk region (BR). This partitioning of the flow is illustrated for the present flow in Fig. 6.

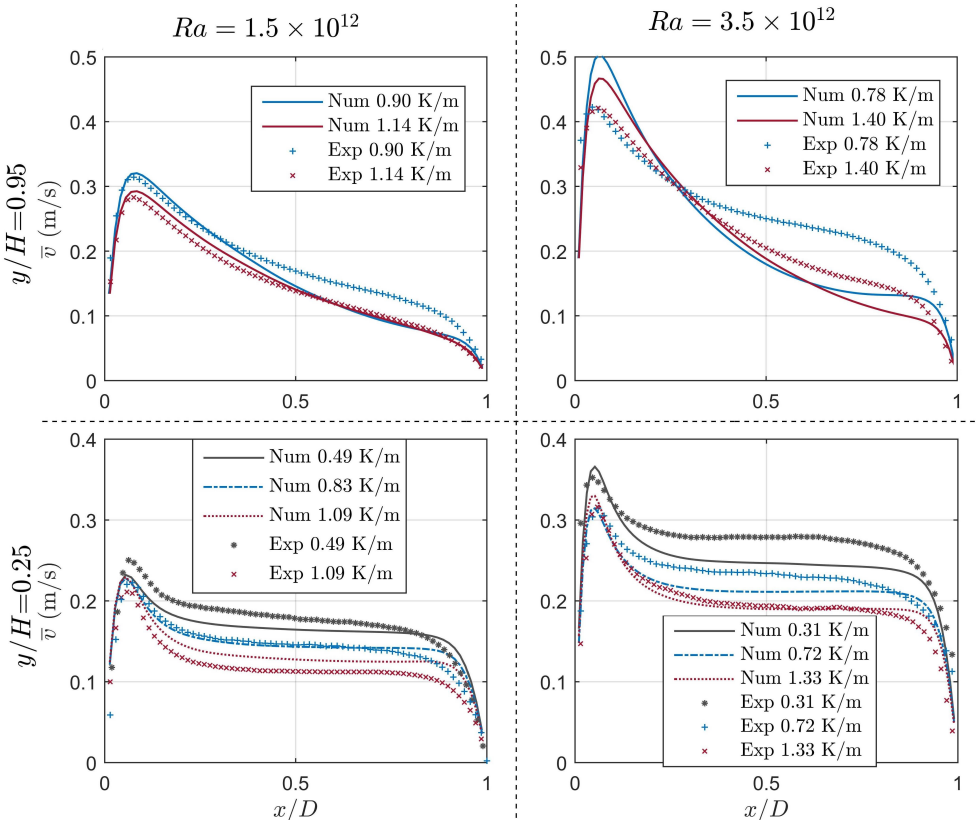

Figure 5: Time averaged velocity profiles at (top) $y/H = 0.95$ and (bottom) $y/H = 0.25$, $z/W = 0.5$, symbols are used for the experimental data while lines are used for numerical results, left $Ra = 1.5 \times 10^{12}$, right $Ra = 3.5 \times 10^{12}$

It can be observed in Fig. 5 that an increase in the external thermal stratification, δ_T results in a decrease of the streamwise velocity similarly to what was observed by Jaluria and Gebhart [9] for a vertical plate. However the velocity profiles are not uniformly changed. Indeed, the peak velocity, in the NCBL, is less affected by the external stratification than the velocity in the BR.

This difference can be explained by the fact that in natural convection flows, the changes in velocities are mainly driven by changes in the buoyant driving forces which themselves depends on the temperatures. However, whereas for no stratification -*i.e.* an isothermal environment- the channel flow exits in an air which is at the same temperature as the inlet temperature, in a positively stratified environment the channel flow exits in an ambient air at higher temperature than the inlet temperature (see schematic representation in Fig. 1 (a)), which tends to oppose the buoyant forces. The outlet temperatures presented in Fig. 4 show that the increase in the external temperature over the channel height stands for nearly 30 to 50 % of the temperature elevation in the BR whereas it represents around 10 % of the temperature in the NCBL. As a consequence the buoyant forces in the NCBL are relatively less impacted by the increase of δ_T than these in the BR, resulting in a least impact on the velocities.

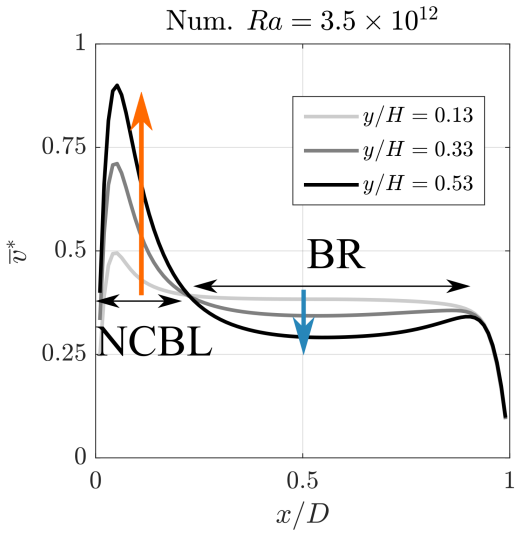

Figure 6: Illustration of the definition of the NCBL and the BR regions. Credit: [7]

Two main conclusions emerged from the experimental and numerical results presented in this section. First, it was observed that as δ_T increased, the velocity was decreased, but the decrease was more pronounced in the BR than in the NCBL. It was also shown that as the external thermal stratification increased, the transition was moved at lower locations in the channel.

4. Extension to weak and negative thermal stratifications

In the following section the numerical model is used to investigate the flow behavior in the cases of weak and negative stratifications. A weak thermal stratification, approaching δ_T=0 K/m, is very hard to establish experimentally especially in a room where the ambient temperature is not controlled. Also, due to its unstable character, a negative stratification of temperature is impossible to obtain in non-controlled laboratory conditions. However, as was mentioned in the introduction, it occurs that in the atmosphere, negative and positive stratifications can be encountered.

Therefore, to investigate these conditions, the effect of the external temperature stratification ranging from $\delta_T \in [-0.5; 1.4]$ K/m on the mass flow rate, the transition behaviour and the maximum temperature reached at the wall were studied numerically with results being presented below.

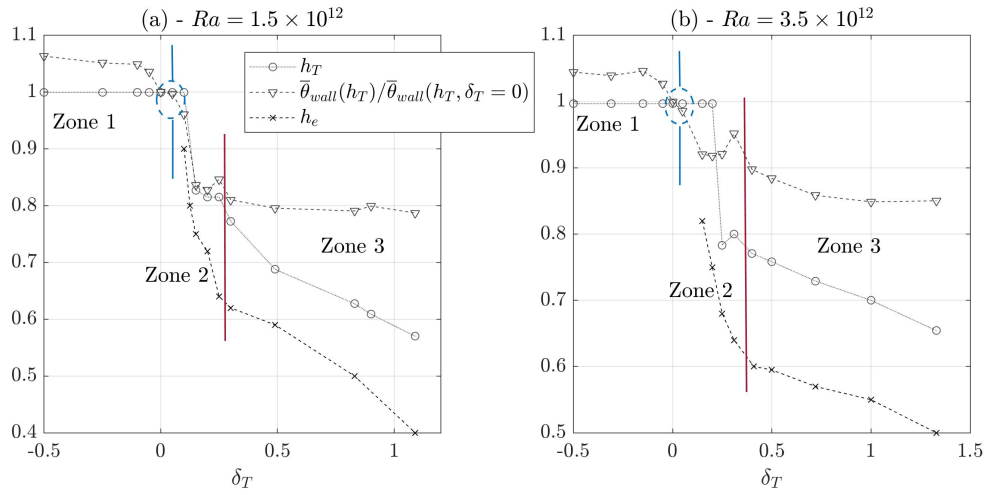

Figure 7: Evolution of h_T, h_e and maximum temperature at the wall for various δ_T at (a) $Ra = 1.5 \times 10^{12}$ and at (b) $Ra = 3.5 \times 10^{12}$

In Fig. 7 (a) and (b), the transition indicators h_e and h_T (defined in section 2.4), and the time-averaged temperature at this height $\overline{\theta}_{wall}(h_T)$ are plotted against δ_T for the cases of $Ra = 1.5 \times 10^{12}$ and $Ra = 3.5 \times 10^{12}$. For visualization purposes $\overline{\theta}_{wall}(h_T)$ was scaled by $\overline{\theta}_{wall}(h_T, \delta_T = 0K/m)$.

As can be seen from Fig. 7, the evolution of h_e, h_T and $\overline{\theta}_{wall}(h_T)$ with δ_T is rather complex. However for both Ra, three zones can be defined in which h_T and $\overline{\theta}_{wall}(h_T)$ have a similar dependence against δ_T.

The first zone corresponds to negative and weak stratifications. Its upper limit, located around $\delta_T \simeq 0$ is difficult to determine with precision, and to that extent has been indicated by an ellipse. In this zone, h_T is at located at y/H=1. Finally, it is not possible to identify h_e in zone 1. As δ_T increases, the second zone is encountered, in which the flow behavior drastically changes. h_T and h_e are displaced to considerably lower levels in the channel and $\overline{\theta}_{wall}(h_T)$ decreases significantly, by up to 25% at $Ra = 1.5 \times 10^{12}$. At both $Ra = 1.5 \times 10^{12}$ and $Ra = 3.5 \times 10^{12}$ there is a peak in h_T and $\overline{\theta}_{wall}(h_T)$ at the end of zone 2. This peak is used as the limit between zone 2 and zone 3. Finally, in zone 3, $\overline{\theta}_{wall}(h_T)$ changes are more predictable and h_e and h_T are displaced lower in the channel almost linearly.

The flow in zone 3 corresponds to this described experimentally and numerically in the previous sections. For this range of stratifications, the flow is transitional and the indicators h_e and h_T, indicating respectively the early and the advanced stages of transition to turbulence, are easily identifiable. This zone is therefore referred to as the transitional zone.

In zone 1, it is not possible to determine h_e which means that transition has not started or that it is at its very early stages. The fact that h_T is at the very top of the channel only means that the maximum temperature is reached at the top of the channel, as it is the case with laminar flows. As a consequence in zone 1, the natural convection flow will be considered as laminar and this zone called the laminar zone. In this zone, the maximum temperature reached at the wall, $\overline{\theta}_{wall}(h_T)$ remains almost constant with a decrease for stratifications approaching 0 K/m.

In zone 2, the flow evolves from a laminar to a transitional flow. The early stages indicator h_e can not be identified for the very first values of δ_T in zone 2 but once h_e appears it becomes possible to observe that the early stages of the transition occur and are displaced lower in the channel as δ_T increases. As for h_T, it remains at the top of the channel for the low values of δ_T in zone 2, even though h_e started to be identifiable. This means that, in these cases, only the early stages of transition have started whereas the advanced stages of transition have not occurred yet within the channel. Then as δ_T increases again, h_T starts to be displaced lower in the channel. This means that the flow go trough the early and the advanced stages of the transition. This zone will be therefore called the Connecting zone.

It can be observed in Fig. 7 (a) that the changes in the maximum temperature reached at the wall can reach 34 % for the investigated range of thermal stratification.

The detailed evolution of the wall temperature distributions as a function of the external thermal stratification and linked to the three different zones defined above can be consulted in the Appendix B.

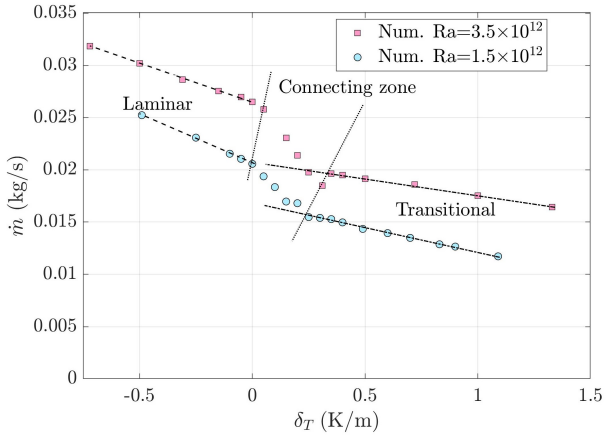

Figure 8: Numerically computed mass flow rate as a function of the external thermal stratification

In Fig. 8, the time and spaced averaged inlet velocities, obtained from the numerical results have been plotted against δ_T. The averaged inlet velocity decreases as the external thermal stratification increases. Moreover, for each Rayleigh number, its evolution can be decomposed in three different regions, delimited here by dotted lines and which are characterized by different dependence to δ_T. The dashed lines were plotted to help visualize the different trends. The three identified regions coincide with the three regions observed in Fig. 7. In Fig. 8, it is easier to determine the limit between the laminar zone and the connecting zone based on velocity changes. This limit will be set at approximately δ_T=0.05 K/m at $Ra = 3.5 \times 10^{12}$ and δ_T=0 K/m at $Ra = 1.5 \times 10^{12}$.

The changes in the mass flow rate and h_T that are observed in the connecting zone are extremely interesting. Indeed, they suggest that, for the same heat input and for rather small variations of the external thermal stratification of 0.2-0.3 K/m, the flow goes from a laminar regime to a transitional regime. Moreover, in the connecting zone, the mass flow rate changes by up to 25% and the maximum temperature by 10 to 20%. A detailed study of the mechanisms that take place in these cases can provide many answers on the onset of transition to turbulence in these type of flows.

For both the Rayleigh numbers a total changes of the mass flow rate by up to 100% can be observed for the investigated range of thermal stratification. This is one of the explanations why the numerical and experimental agreements of transitional flow have never been reached in these configuration. Indeed, since in the literature works, δ_T was not modeled in numerical studies the experimental and numerical data could not be made to match when thermal stratification was present during the experimental measurements.

As can be seen, in Figs. 8 and 7 (and in Appendix B), it is possible to model the non-stratified case numerically. The cases without stratification actually corresponds to what was previously done in numerical studies of the literature (exception of Ramalingom et al. [15], as mentioned in the introduction). As a matter of fact, for this specific channel configuration, and Rayleigh number, Lau et al. [31] conducted a study without stratification in which they attempted obtaining closer agreement with experimental by increasing inlet disturbance level. However as was mentioned at the beginning of Section 3, there are large discrepancies between the literature results, and therefore, no benchmark solution of a transitional flow makes consensus yet. For this reason, neither the results nor those of Lau et al. [31] can be compared to a reference non-stratified case of the literature.

5. Prediction of the impact of the thermal stratification on the mass flow rate

In an experimental and theoretical paper [20], the present authors proposed a simple one-dimensional theory for modelling and predicting the impact of thermal stratification on the convective mass flow rate in vertical channel. This model was validated against experimental data from the authors and from the literature [18] obtained in an air and a water channel. However, only experimental data was available so that the cases of weak and negative thermal stratification were not studied. The aim of this section is to assess the viability of this model to predict the influence of δ_T on the mass flow rate calculated from the present numerical results, which includes weak and negative thermal stratification.

The theory of Thebault et al. [20] leads to the relation

$$\frac{\dot{m}}{\dot{m}_{ref}} = \frac{1}{1 + S_T}, \tag{5}$$

in which S_T is given by

$$S_T = \frac{H\delta_T - \Delta T_{in} + \Delta T_{out}}{\Delta T_{ref}}, \tag{6}$$

the subscript ref refers to a reference case in which the atmosphere is not stratified ($\delta_T = 0$). ΔT_{ref} is the temperature rise of the fluid in the channel in the reference case, estimated from the simplified energy balance of the channel,

$$Q = \dot{m}_{ref} C_p \Delta T_{ref}, \tag{7}$$

where Q (W) is the total heat input, C_p ($\mathrm{m}^2 \cdot \mathrm{kg} \cdot \mathrm{s}^{-2} \cdot \mathrm{K}^{-1}$) is the specific heat capacity of air, ΔT_{in} is the temperature difference between the air entering the channel inlet and the temperature at the same height of the channel inlet but in the ambient fluid far-field, T_0. ΔT_{out} is the temperature difference between the air in the surrounding of the channel outlet and the temperature at the same height but in the ambient fluid far-field. More details about the definition of ΔT_{in} and ΔT_{out} are presented in Thebault et al. [20]. In the numerical results, ΔT_{out} and ΔT_{in} are found to vary linearly with $H\delta_T$ and their values are presented in Table 2.

Table 2: Parameters of the theoretical model

	Laminar zone			Transitional zone		
Ra	ΔT_{inlet}	ΔT_{outlet}	$\dot{m}_{ref}$	ΔT_{in}	ΔT_{out}	$\dot{m}_{ref}$
1.5×10^{12}	-0.21$H\delta_T$	0.07$H\delta_T$	0.0205	-0.21$H\delta_T$	0.28$H\delta_T$	0.0167
3.5×10^{12}	-0.23$H\delta_T$	0.10$H\delta_T$	0.0264	-0.23$H\delta_T$	0.27$H\delta_T$	0.0210

Another crucial parameter of the predictive model is the evaluation of $\dot{m}_{ref}$ which corresponds to the mass flow rate in the channel in the reference case, *i.e.* when there is no stratification. In the study of Thebault et al. [20], it was not possible to experimentally measure $\dot{m}_{ref}$ because the external thermal stratification was always positive. As a consequence its value was obtained by extrapolation of the experimental data. However, in their experimental data, the flow was always transitional with as can be seen in Fig. 9, where h_T is plotted as a function of δ_T, for all the experimental cases that they used.

In the present study, it can be seen in Fig. 8 that an extrapolation of the numerically obtained mass flow rates raises an issue. Indeed the $\dot{m}_{ref}$ that can be calculated from an extrapolation of the mass flow rates of the

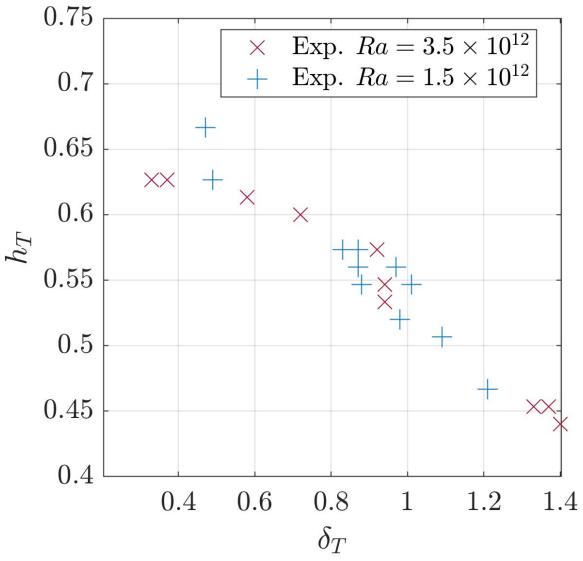

Figure 9: Evolution of h_T for the various δ_T used in the work of Thebault et al. [20]

transitional zone does not coincide with the $\dot{m}_{ref}$ obtained numerically for $\delta_T = 0$.

Because the theory of Thebault et al. [20] did not considered changes in the flow configuration, two different $\dot{m}_{ref}$ are used in the present paper depending on whether the flow is in the laminar or the transitional zone. The reference mass flow rate for the laminar flow configurations, $\dot{m}_{ref,lam}$, corresponds to the value obtained numerically at $\delta_T = 0$ K/m. The reference mass flow rate for the transitional zone $\dot{m}_{ref,tran}$, is evaluated from a linear extrapolation of the numerically obtained mass flow rate in this zone (Fig. 8). Finally, the points in the connecting zone were disregarded in what follows as neither $\dot{m}_{ref,lam}$ nor $\dot{m}_{ref,tran}$ yielded a good result. This was expected as complex phenomena occur in this zone that strongly alter the flow behaviour.

The non-dimensional mass flow rates scaled by $\dot{m}_{ref,lam}$ or $\dot{m}_{ref,tran}$ have been plotted against S_T in Fig. 10. The experimental data of Thebault et al. [20] were reported as well. As can be seen, the theoretical model predicts precisely the mass flow rates for the laminar and transitional zones with differences below 1%.

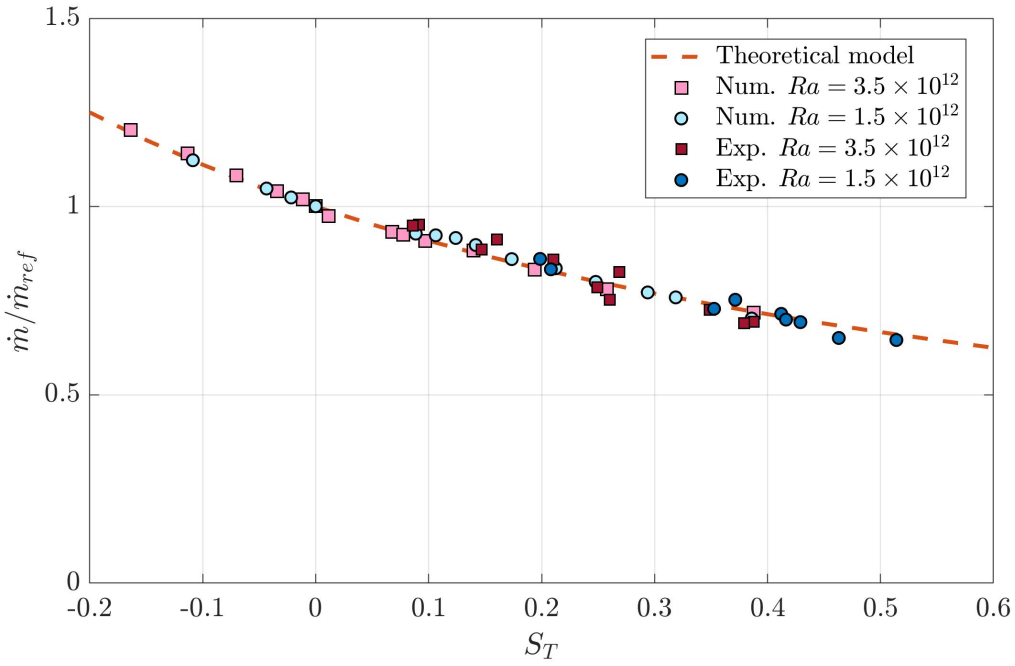

Figure 10: Non-dimensional mass flow rated plotted against the stratification parameter S_T. Pink squares - Numerical 230 W, Light Blue circles Numerical - 100 W, Red squares - Experimental 230 W, Dark Blue circles Experimental - 100 W, the orange dotted lines plots the analytical solution

6. Conclusion

The effect of the external thermal stratification on a transitional natural convection flow in a channel was studied experimentally and numerically. Positive stratifications were studied experimentally whereas positive and negative stratifications were studied numerically. Two heat inputs were investigated namely 90 W/m^2 and 208 W/m^2, which correspond to Rayleigh numbers of of $Ra = 1.5 \times 10^{12}$ and $Ra = 3.5 \times 10^{12}$. To model the experimental ambient temperature distribution, a stratification of temperature and pressure was considered at the open boundaries of the computational domain.

There is a remarkable agreement in trends between the experimental and numerical results regarding the effect of the external thermal stratification on the time averaged velocities in the inlet and outlet regions of the chan-

nel as well as on the time-averaged temperatures at the heated wall and at the outlet. The effect of the external thermal stratification on the transitional behavior of the flow is also well captured numerically. It was observed experimentally and numerically, that an increase in the external thermal stratification induces:

1. a decrease of the mass flow rate. However the peak velocity, near the heated wall is less impacted than the bulk flow velocities,
2. a decrease of the maximum temperature reached at the wall,
3. a displacement of the location of the transition to a lower elevation of the channel.

This last point is explained by the fact that, as the external thermal stratification increases larger shear stresses are produced in lower regions of the channel, moving the transition to a lower location.

The numerical model is then used to study the cases of weak and negative stratification which are commonly encountered in the first meters of the atmosphere. Three flow behaviors were identified depending on the stratification parameter: a laminar zone for negative and very weak stratifications and in which no transition of the flow is observed, a connecting zone for weakly positive stratifications in which the flow changes from a laminar flow to a transitional flow, and finally a transitional zone for higher positive stratification in which transition to turbulence occurs within the channel.

It is shown that an increase of the external positive upward thermal gradient provokes a decrease of the mass flow rate whereas rise in the magnitude of a negative upward external thermal gradient causes an increase in the mass flow rate.

Numerically the changes in the mass flow rate and the maximum wall temperature can change by up to 100% and 34% respectively between the highest and lowest investigated stratifications. Experimentally a change in stratification by 1 K/m yields a change in the mass flow rate by 35%.

It is now clear that the thermal stratification is a crucial parameter in such studies. It also explains, at least in part, the difficulties experienced in achieving repeatability in experimental measurements under supposedly identical conditions as well as the difficulty to perform numerical experimental confrontations.

Finally there is an excellent agreement between the theoretical mass flow rate prediction developed in earlier work [20] and the numerical data with positive and negative upward external thermal gradients.

Acknowledgement
The authors would like to thanks Svetlana Tkachenko and Oksana Tkachenko as well as Adrian Vieri for their help and contribution to setting up the numerical model. Thanks to Yohann Duguet for its insights on transitional flows. My acknowledgement to the InnoEnergy PhD School Programme and to the European Institute of Technology (EIT) for the financial support provided during my international mobility.

Appendix A. Mechanisms of the displacement of the transition in a channel flow with various δ_T

Despite that the transitional processes in natural convection flow induced by hot vertical plates have not been fully explained yet, it is commonly accepted to consider that shear stresses are one of the driving factors that triggers transition to turbulence (see e.g. [11, 23, 19, 7]).

In the present work it was observed (section 3, Fig. 5) that as δ_T increased, the velocity difference between the NCBL and the BR, and therefore the shear stresses, also increased lower in the channel. As a result, the transition to turbulence, triggered by the shear stresses, is also displaced at lower locations in the channel as δ_T increases.

Now, as was mentioned in the introduction, in an isoflux vertical plate configuration, Jaluria and Gebhart [9] observed that, as the external thermal stratification increased, the transition was postponed at higher locations in the channel. This observation may seem contradictory with what is observed here in a vertical channel. But if the shear stresses are considered as the main driver for this transition, it is possible to explain these opposite trends. Indeed, in the case of vertical plates the flow far enough from the heated plate is not moving. Consequently, the shear stresses only results from the high velocity region near the heated plate. Given that the increase of the external thermal stratification also decreases the velocity in the case of vertical plates [9], it therefore decreases the shear stresses, and consequently, displaces the transition at higher locations.

The behaviors for both the channel and the vertical plates are illustrated in Fig. .11 (a) and (b) respectively. To sum up, in channel flow, the increase of δ_T increases the velocity difference between the high velocity region and the low velocity region, increasing the shear stresses therefore leading to a displacement of the transition upstream. In vertical plate flow, the increase of δ_T decreases the velocity differences between the high velocity region and

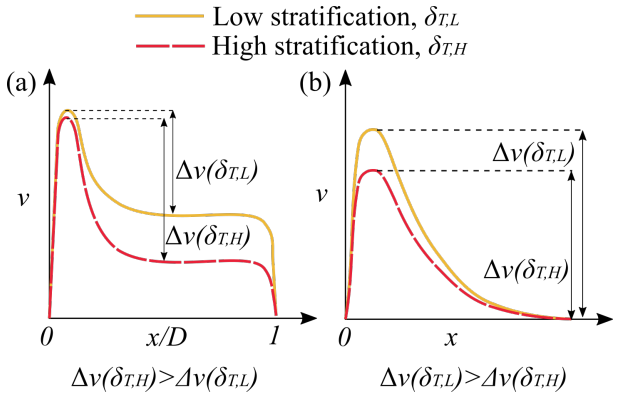

Figure .11: Schematic representation of the evolution of the streamwise velocity distributions, and the velocity difference Δv between the high velocity region and the low velocity region at a fixed elevation y and for two external thermal stratifications, a low stratification $\delta_{T,L}$ and a high stratification $\delta_{T,H}$, (a) vertical channel, (b) vertical plate.

the still freestream flow, therefore reducing the shear stresses, displacing transition at higher locations.

Note that other phenomena, not investigated here, may also contribute to the transition phenomena. Despite the fact that in the present configuration no permanent flow reversals were observed, an intermittent flow is present as was demonstrated by Sanvicente et al. [21], and may play a role in the destabilization processes. Jannot and Kunc [37] also claim that the onset of transition in the case of natural convection induced by isothermal vertical plates, originates from the interaction between characteristic traveling wave within the boundary layer and the Brunt-Väisälä frequency, inherent to thermally stratified environment. Also note that, in the present configuration, a positive δ_T induces an adverse pressure gradient (equation 3) at the boundaries of the channel. To the best of our knowledge, the effect of adverse pressure gradient has not been studied for the case of natural convection boundary layer. However, in the case of wall-bounded forced flow (not buoyancy driven) an adverse pressure gradient decreases the flow velocities but also triggers the transition at lower locations (see e.g. [38]). It is therefore interesting to note that in the present natural convection channel flow, the effect of the temperature stratification - and the inherent pressure stratification which is somehow similar to an adverse pressure gradient - is in coherence with what was observed with adverse pressure gradient in wall-bounded transitional boundary layer.

Appendix B. Time-averaged velocity and wall temperatures distributions for various δ_T

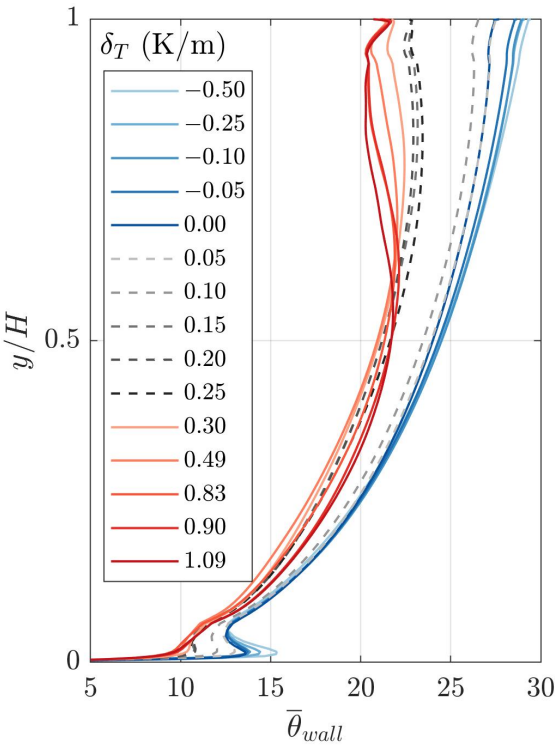

Figure .12: Time-averaged wall-temperature in the mid-plane at z/W=0.5 for various external thermal stratification at $Ra = 1.5 \times 10^{12}$

The time-averaged wall temperatures for negative and positive δ_T at $Ra = 1.5 \times 10^{12}$ have been plotted in Fig. .12. Three set of colors were used. Blue colors are used for wall temperature in the laminar zone, dashed grey lines are used for the connecting zone and the red lines are used for the transitional zone.

In the laminar zone, the values of the wall temperatures increase up to the top of the channel which is typical for laminar natural convection flow. Some slight changes are observed in the very top of the channel which may be due to exit effect as were already reported in previous studies (see e.g. [21]). It is also seen that there is a temperature peak in the bottom part of the channel.

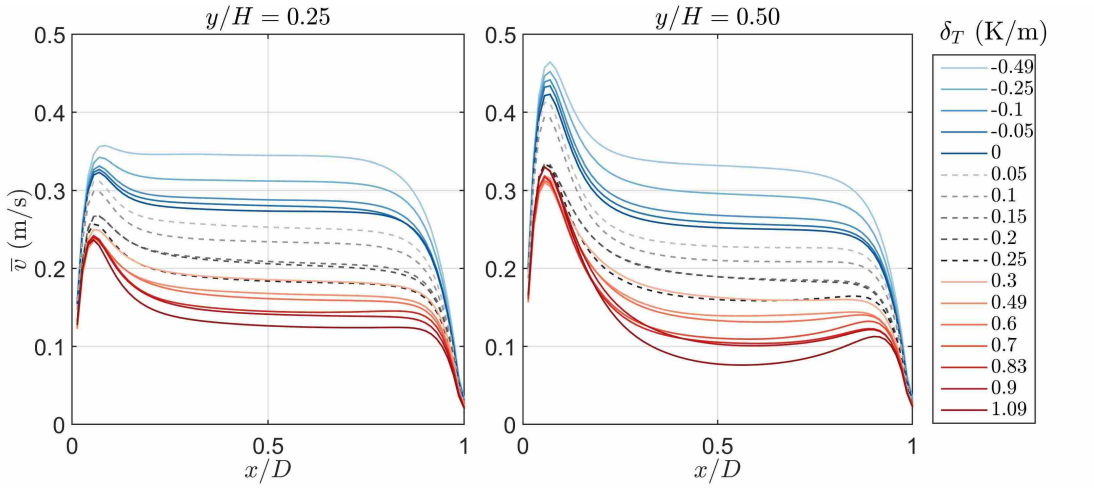

Figure .13: Time-averaged velocity in the mid-plane at z/W=0.5 and at heights y/H=0.25, y/H=0.5 for various external thermal stratification at $Ra = 1.5 \times 10^{12}$.

This is due to the separation of streamlines which occurs at the leading edge. In this area, a local recirculation is created which induces a local rise of temperature. This phenomenon have already been observed experimentally and numerically (see e.g. [39]). It can be noted that for the laminar zone, the wall temperature rises as δ_T decreases. This could be in part due to the fact that, when there is a negative thermal stratification, the air below the entrance of the channel is at a higher temperature than T_0. Consequently, as the external thermal stratification decreases, the temperature of the air entrained inside the channel increases which slightly heats up the fluid in the channel. In the connecting zone, the wall temperature profiles progressively evolve from a profile of a laminar channel flow to the one of a transitional regime.

Time-averaged velocity profiles at y/H=0.25 and y/H=0.50 have been plotted in Fig. .13. The profiles are similar to those previously described with variation in the BR and NCBL velocities.

Contrary to the velocity profiles of the transitional zone for which the BR is more affected by the changes in δ_T than the NCBL region (see section 3), it is not as pronounced for the velocity profiles of the connecting and the laminar zones.

References

[1] M. H. Esteki, J. Reizes, M. Behnia, Natural convection heat transfer from electronic components located in an enclosure, International Journal of Fluid Mechanics Research 25 (1998) 711–719.

[2] E. E. Zukoski, Review of flows driven by natural convection in adiabatic shafts, NASA (1995).

[3] K. Seo Young, J. Yogesh, Basic considerations in combined buoyancy-induced and forced flow in a vertical open shaft, Numerical Heat Transfer, Part A: Applications 34 (1998) 519–536. doi:10.1080/10407789808914001.

[4] F. Allard, F. Allard, Natural ventilation in buildings: a design handbook, James & James London, 1998.

[5] D. Yang, T. Du, S. Peng, B. Li, A model for analysis of convection induced by stack effect in a shaft with warm airflow expelled from adjacent space, Energy and Buildings 62 (2013) 107–115.

[6] J. Bloem, Evaluation of a pv-integrated building application in a well-controlled outdoor test environment, Building and Environment 43 (2008) 205–216.

[7] M. Thebault, S. Giroux-Julien, V. Timchenko, C. Ménézo, J. Reizes, Detailed flow development and indicators of transition in a natural convection flow in a vertical channel, International Journal of Heat and Mass Transfer 143 (2019) 118502.

[8] R. Cheesewright, Natural convection from a plane, vertical surface in non-isothermal surroundings, International Journal of Heat and Mass Transfer 10 (1967) 1847–1859.

[9] Y. Jaluria, B. Gebhart, Stability and transition of buoyancy-induced flows in a stratified medium, Journal of Fluid Mechanics 66 (1974) 593–612.

[10] M. Miyamoto, Y. Katoh, J. Kurima, H. Sasaki, Turbulent free convection heat transfer from vertical parallel plates., in: The Eighth International Heat Transfer Conference, volume 4, Hemisphere Publishing Corporation, 1986, pp. 1593–1598.

[11] T. Kogawa, J. Okajima, A. Komiya, S. Armfield, S. Maruyama, Large eddy simulation of turbulent natural convection between symmetrically heated vertical parallel plates for water, International Journal of Heat and Mass Transfer 101 (2016) 870–877.

[12] C. Garnier, Modélisation numérique des écoulements ouverts de convection naturelle au sein d'un canal vertical asymétriquement chauffé, Phd thesis, Université Pierre et Marie Curie, 2014.

[13] A. Zoubir, Étude des transferts thermo-convectifs dans un canal semi-ouvert : Application aux façades type double-peau, Phd thesis, INSA de Lyon, 2014.

[14] C. Hemmer, C. Popa, A. Sergent, G. Polidori, Heat and fluid flow in an uneven heated chimney, International Journal of Thermal Sciences 107 (2016) 220–229.

[15] D. Ramalingom, P. Cocquet, B. A., Numerical study of natural convection in asymmetrically heated channel considering thermal stratification and surface radiation, Numerical Heat Transfer, Part A: Applications 72 (2017) 681–696.

[16] W. Haaf, K. Friedrich, G. Mayr, J. Schlaich, Solar chimneys part i: Principle and construction of the pilot plant in manzanares, International Journal of Solar Energy 2 (1983) 3–20.

[17] H. Flohn, R. Penndorf, The stratification of the atmosphere (i), Bulletin of the American Meteorological Society 31 (1950) 71–78.

[18] C. Daverat, H. Pabiou, H. Bouia, S. Xin, C. Ménézo, Convection naturelle dans un canal vertical en eau avec chauffage pariétal : influence de la stratification., in: 20ième Congrès Français de Mécanique, 20, Presses universitaires de Franche-Comté, 2011, pp. 162–167.

[19] Y. Li, C. Daverat, H. Pabiou, C. Ménézo, S. Xin, Transition to turbulent heat transfer in heated vertical channel - scaling analysis, International Journal of Thermal Sciences 112 (2017) 199–210.

[20] M. Thebault, J. Reizes, S. Giroux-Julien, V. Timchenko, C. Ménézo, Impact of external temperature distribution on the convective mass flow

rate in a vertical channel–a theoretical and experimental study, International Journal of Heat and Mass Transfer 121 (2018) 1264–1272.

[21] E. Sanvicente, S. Giroux-Julien, C. Ménézo, H. Bouia, Transitional natural convection flow and heat transfer in an open channel, International Journal of Thermal Sciences 63 (2013) 87–104.

[22] G. Polidori, S. Fatnassi, R. Ben Maad, S. Fohanno, F. Beaumont, Early-stage dynamics in the onset of free-convective reversal flow in an open-ended channel asymmetrically heated, International Journal of Thermal Sciences 88 (2015) 40–46.

[23] C. Daverat, Y. Li, H. Pabiou, C. Ménézo, S. Xin, Transition to turbulent heat transfer in heated vertical channel - experimental analysis, International Journal of Thermal Sciences 111 (2017) 321–329.

[24] Y. Li, H. Pabiou, C. Ménézo, Unsteady heated vertical channel flow in a cavity, International Journal of Thermal Sciences 125 (2018) 293–304.

[25] O. Manca, B. Morrone, V. Naso, A numerical study of natural convection between symmetrically heated vertical parallel plates, in: XII Congresso Nazionale UIT, 1994, pp. 379–390.

[26] G. E. Lau, G. H. Yeoh, V. Timchenko, J. A. Reizes, Application of dynamic global-coefficient subgrid-scale models to turbulent natural convection in an enclosed tall cavity, Physics of Fluids 24 (2012) 094105.

[27] G. E. Lau, G. H. Yeoh, V. Timchenko, J. A. Reizes, Large-eddy simulation of natural convection in an asymmetrically-heated vertical parallel-plate channel: Assessment of subgrid-scale models, Computers & Fluids 59 (2012) 101–116.

[28] C. Daverat, H. Pabiou, C. Ménézo, H. Bouia, S. Xin, Experimental investigation of turbulent natural convection in a vertical water channel with symmetric heating: Flow and heat transfer, Experimental Thermal and Fluid Science 44 (2013) 182–193.

[29] M. Thebault, Coherent structures and impact of the external thermal stratification in a transitional natural convection vertical channel, Theses, Université de Lyon ; University of New South Wales, 2018. URL: https://tel.archives-ouvertes.fr/tel-02006828.

[30] A. G. Fedorov, R. Viskanta, Turbulent natural convection heat transfer in an asymmetrically heated, vertical parallel-plate channel, International Journal of Heat and Mass Transfer 40 (1997) 3849–3860.

[31] G. E. Lau, V. Timchenko, C. Ménézo, S. Giroux-Julien, M. Fossa, E. Sanvicente, J. A. Reizes, G. H. Yeoh, Numerical and experimental investigation of unsteady natural convection in a vertical open-ended channel, Computational Thermal Sciences: An International Journal 4 (2012).

[32] A. Smirnov, S. Shi, I. Celik, Random flow generation technique for large eddy simulations and particle-dynamics modeling, Journal of Fluids Engineering 123 (2001) 359–371.

[33] G. R. Tabor, M. H. Baba-Ahmadi, Inlet conditions for large eddy simulation: A review, Computers & Fluids 39 (2010) 553–567.

[34] C. Li, M. Tsubokura, W. Fu, N. Jansson, W. Wang, Compressible direct numerical simulation with a hybrid boundary condition of transitional phenomena in natural convection, International Journal of Heat and Mass Transfer 90 (2015) 654–664.

[35] O. A. Tkachenko, V. Timchenko, S. Giroux-Julien, C. Ménézo, G. H. Yeoh, J. A. Reizes, E. Sanvicente, M. Fossa, Numerical and experimental investigation of unsteady natural convection in a non-uniformly heated vertical open-ended channel, International Journal of Thermal Sciences 99 (2016) 9–25.

[36] G. E. Lau, G. H. Yeoh, V. Timchenko, J. A. Reizes, Large-eddy simulation of turbulent natural convection in vertical parallel-plate channels, Numerical Heat Transfer, Part B: Fundamentals 59 (2011) 259–287.

[37] M. Jannot, T. Kunc, Onset of transition to turbulence in natural convection with gas along a vertical isotherm plane, International Journal of Heat and Mass Transfer 41 (1998) 4327–4340.

[38] B. Abu-Ghannam, R. Shaw, Natural transition of boundary layers—the effects of turbulence, pressure gradient, and flow history, Journal of Mechanical Engineering Science 22 (1980) 213–228.

[39] J. Vareilles, Étude des transferts de chaleur dans un canal vertical différentiellement chauffé : application aux enveloppes photovoltaïques/thermiques, Phd thesis, Université Claude Bernard Lyon 1, 2007.